PASJ: Publ. Astron. Soc. Japan **54**, 223–228, 2002 April 25

Spiral Molecular Front in Galaxies: Quick Transition from Atomic to Molecular Hydrogen in Spiral Arms

Makoto HIDAKA and Yoshiaki SOFUE
Institute of Astronomy, The University of Tokyo, Mitaka, Tokyo 181-0015
sofue@ioa.s.u-tokyo.ac.jp

(Received 2001 October 25; accepted 2002 February 8)

Abstract

We derived a two-dimensional map of the molecular fraction, $f_{\rm mol}$ (ratio of the molecular gas density to that of total gas), in the spiral galaxy M 51, and examined the behavior of molecular fronts (MF), where MF denotes the place where $f_{\rm mol}$ changes drastically from nearly zero to unity, and vice versa. We showed that the MF phenomenon is not only radial, but also occurs in the azimuth direction through the spiral arms, and $f_{\rm mol}$ changes rapidly in the arm-to-interarm transition regions. The existence of the azimuthal MF indicates that the atomic gas (H I) is quickly transformed to molecular gas (H_2) during passage through spiral arms. We performed a numerical simulation of MF based on an H I-to-H_2 phase-transition theory, and reproduced the observations. We estimated the azimuthal scale length of the transition to be less than 200 pc, corresponding to a time scale of ~ 2 Myr for H_2 gas formation. The azimuthal width of a molecular arm was estimated to be at most 2.5 kpc, where the gas can remain in the molecular phase for about 25 Myr.

Key words: galaxies: cluster of — galaxies: ISM — galaxies: spiral — H I gas — molecular gas

1. Introduction

Neutral (H I) and molecular (H_2) hydrogen gases are the two major components of the interstellar matter. Elmegreen (1993) has proposed a simple model to predict the molecular fraction by assuming a quasi-static equilibrium between the two phases in individual interstellar clouds. However, the dynamical transition between the H I and H_2 gas phases are not well understood in real galaxies. Are giant molecular clouds (GMC) long-lived clouds living for several galactic rotations while crossing the spiral arms many times, and coexisting with the H I gas? Alternatively, are they formed quickly from H I gas when the interarm H I encounters the arms, and does molecular gas return to H I again, when going out of the arms?

These questions can be answered by studying the distribution of the molecular fraction (the ratio of molecular-gas density to the total gas density) in the gas disk of spiral galaxies. Global variations of the molecular fraction in disk galaxies were obtained by our earlier studies (Sofue et al. 1995; Honma et al. 1995), in which we applied the Elmegreen's theory of atomic-to-molecular gas transitions. We showed that the inner gas disk is dominated by molecular gas, while the outer disk is dominated by H I, and the transition between H I and H_2 occurs in a narrow annulus in the disk, across which the molecular fraction varies drastically. We call this transition region the "molecular front (MF)". Such a front phenomenon was also found in the direction perpendicular to the galactic plane, so that the H_2 disk is sandwiched by a fat H I disk (Imamura, Sofue 1997). However, these analyses do not tell us about the dynamics and time scale of the H I-to-H_2 transition.

In the present work, we investigated the MF phenomenon across spiral arms by obtaining a two-dimensional distribution of molecular fraction in a galactic disk. The azimuthal variation of the molecular fraction across spiral arms provide information about the dynamical evolution of the H I–H_2 phase transition and molecular gas formation in spiral arms.

2. Molecular Front

2.1. Radial and Vertical Molecular Front

Many observations of neutral hydrogen and molecular gas have been carried out, and have revealed two important aspects. First, the neutral hydrogen gas is broadly distributed in the disk, and is often extended outside the optical disks, while it is deficient in the central regions. On the other hand, molecular gases are concentrated in the central few kpc regions. The radial variations of the distributions of H I and H_2 gases have been quantified by analyzing the molecular fraction as a function of the galacto-centric distance. The molecular fraction, $f_{\rm mol}$, is defined by

$$f_{\rm mol} = \frac{\rho({\rm H}_2)}{\rho({\rm HI})} + \rho({\rm H}_2) = \frac{2 \times n({\rm H}_2)}{n({\rm HI})} + 2 \times n({\rm H}_2). \quad (1)$$

Sofue et al. (1995) have investigated radial variation of the molecular fraction in several spiral galaxies. They found that the molecular fraction is almost unity in the central few kpc region, and decreases suddenly at a certain radius to be almost zero, beyond which the gas is almost totally in the H I phase.

Honma et al. (1995) modeled the MF by applying the phase transition theory of Elmegreen (1993). According to this theory, the molecular fraction is determined by three parameters: the interstellar pressure, P; the UV radiation field, U; and the metallicity, Z. Honma et al. showed that, if these three parameters are approximated by exponential functions of galacto-centric radius, the observed molecular front in the radial direction can be well reproduced. They applied this model to several real galaxies, and obtained good coincidence with the observed data.

Spiral galaxies have density waves and spiral arms. Because the spiral pattern speed is much slower than the gas rotation, the gases collide with the spiral potential, resulting in galactic shock waves, where the gas density and pressure increase suddenly. The compression results in star formation, leading to an increase of the radiation-field intensity. Thus, the MF parameters, (P, U, Z), will vary as a function of the azimuthal angle, which may result in another type MF spatially correlated with the spiral arms. In order to investigate the existence of such spiral MF, we first examined the H I and CO-line data from the literature, and constructed a 2D map of the molecular fraction in M 51. We, then, performed numerical simulation using the transition model established by Elmegreen (1993), and made a comparison with the observations.

2.2. *Spiral Molecular Front in M 51: Azimuthal Variation of Molecular Fraction*

For obtaining a two-dimensional map of the molecular fraction, we made use of the data from the literature that provided sufficient angular resolution in both H I and CO. Here, we chose the 'grand-design' spiral galaxy NGC 5194 (M 51), which was also studied in Honma et al. (1995). We used the ^{12}CO (J = 1–0) imaging data obtained with the Nobeyama 45-m telescope (Nakai et al. 1994) with a beam width of $16''$ and a grid spacing of $15''$, corresponding to an angular resolution of $24''$, and the H I data obtained with the VLA at $34'' \times 34''$ resolution from Rots et al. (1990). Integrated-intensity maps of H I and CO are shown in figure 1 at the same resolution of $34''$. These two maps reveal the typical behavior of atomic and molecular hydrogen gases: H I is extended broadly in the disk, having a central deficient, while CO is concentrated in the central region.

We calculated the column density of H I and H_2 from the integrated intensity, adopting the following relation between the column density and intensity:

$$n(\mathrm{H\,I}) = C(\mathrm{H\,I}) \times I(\mathrm{H\,I}), \tag{2}$$

$$n(\mathrm{H_2}) = C(\mathrm{CO}) \times I(\mathrm{CO}), \tag{3}$$

where C(H I) and C(CO) are the conversion factors. The value of C(H I) was taken as $1.82 \times 10^{18}\,\mathrm{cm^{-2}\,K^{-1}\,km^{-1}\,s}$. In order to estimate the amount of the total molecular gas mass from the CO intensity, we adopted a conversion factor of $C(\mathrm{CO}) = 1.1 \times 10^{20}\,\mathrm{cm^{-2}\,K^{-1}\,km^{-1}\,s}$ from Arimoto et al. (1996), and assumed no radial dependence of the conversion factor. The difference of the angular resolution was corrected, so that both H I and CO maps would have the same resolution of $34''$; also the grid separation was corrected by using a bicubic interpolation. Using equation (1), we calculated the molecular fraction; a two-dimensional distribution map of the molecular fraction is shown in figure 2.

Figure 2 shows that the molecular fraction is almost unity in the central $r < 60''$ region, or at $r < 2.8$ kpc. Toward the northwest and southeast, where the bisymmetric spiral structure is not clearly seen in both the H I and CO distributions, the molecular fraction decreases drastically to zero at $r > 110''$, or $r > 5.1$ kpc. This sudden radial decrease of the molecular fraction confirms the radial MF at $r \sim 5$ kpc.

In the northeast and southwest, where the molecular spiral arms are prominent, a high-f_{mol} region extends out to ~ 7 kpc. In the southeast direction, f_{mol} suddenly decreases to 0.6 at $r \sim 60''$, and increases again to a value greater than 0.9, and finally decreases to zero. This re-increase of the molecular fraction results from the spiral arms, as already mentioned by Kuno et al. (1995).

Figure 2 shows that the molecular front exists along the spiral arms in addition to the global radial variation. This implies that the circularly flowing gas experiences quick transitions from atom to molecule by encountering the spiral arms, and from molecule to atom when going out from the spiral arms. However, the present angular resolution is not high enough to investigate the scale length of the variation across the arms in more detail. We can estimate only the upper limit of the scale length, which is about 700 pc in the azimuthal direction. Since the rotation velocity is about $200\,\mathrm{km\,s^{-1}}$ (Kuno, Nakai 1997) and the pattern speed of the density waves would be $\sim 20\,\mathrm{km\,s^{-1}\,kpc^{-1}}$, the upper limit of time scale of atom-to-molecule and molecule-to-atom phase transitions is estimated to be several Myr.

3. Simulation of the Molecular Front

3.1. *Numerical Methods*

In the previous section, we showed the existence of MF in the azimuthal direction. However, because of poor angular resolution, we could not estimate the exact MF scale length in the arms. Here, we try to estimate the scale length based on numerical simulations. The azimuthal variances of the gas density was calculated using the hydrodynamical code, not taking into account of the self-gravity of the gas. The variation of metallicity and radiation field was assumed to have an axisymmetric exponential distribution, as adopted by Honma et al. (1995), but no azimuthal variation was assumed.

For calculating the gas dynamical behavior of the disk, we used the freely downloadable and usable hydrodynamical code, VH-1 (Blondin, Lufkin 1993). This is a multidimensional hydrodynamics code for an ideal compressible fluid written in FORTRAN, and developed by a numerical astrophysics group at the University of Virginia based on the Piecewise Parabolic Method Lagrangian Remap (PPMLR) scheme of Colella and Woodward (1984). The PPMLR has the advantage of maintaining contact discontinuities without the aid of a contact steepener, and can be well applied to a galactic-scale hydrodynamical simulation. The code does not include self-gravity, artificial viscosity, variable γ equation of state, and radiative heating and/or cooling. Hence, we assume that the interstellar gas is ideal, inviscid, and compressible.

3.1.1. *Gravitational potential*

In order to simulate the evolution of the spiral structure in the gas disk, we assumed a given gravitational potential, which comprises the following two terms: (i) a static axisymmetric potential, and (ii) a nonaxisymmetric, rotating bar potential. The self-gravity of the gas was not taken into account. The potential is expressed by

$$\Phi(R, \phi) = \Phi_0(R) + \Phi_1(R, \phi). \tag{4}$$

We adopted a "Toomre disk" (Toomre 1981) potential for the

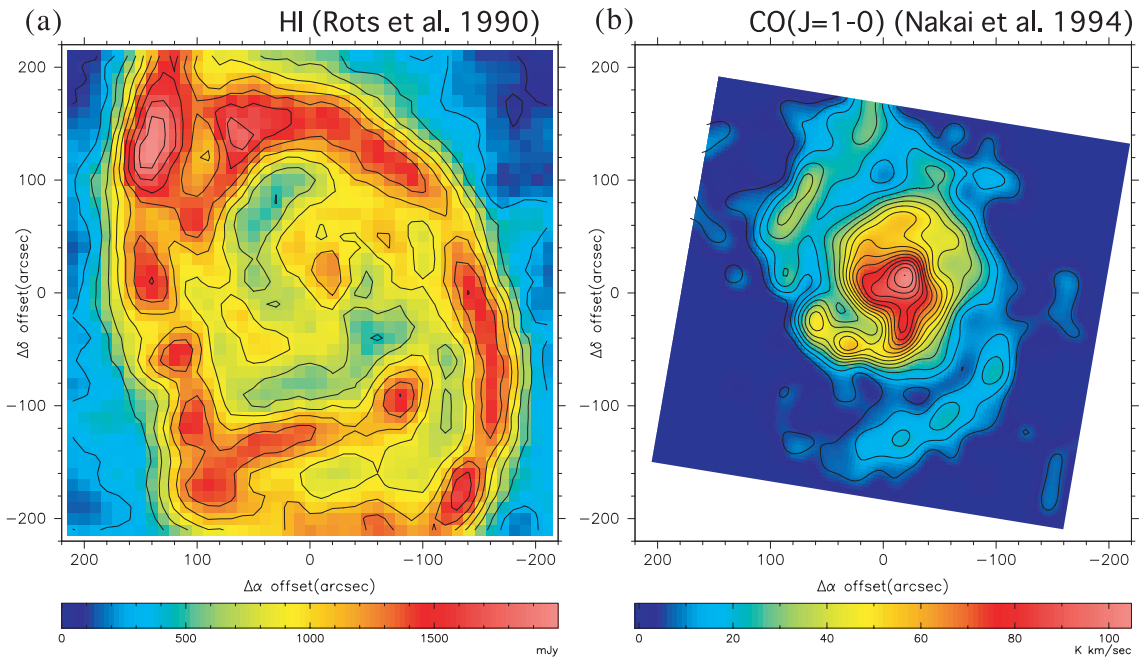

Fig. 1. (a) H I integrated-intensity map of NGC 5194 (M 51) at 34″ resolution (Rots et al. 1990). The contour levels are 100, 300, 500, ..., and 1900 mJy/beam and the intensity key is shown at the bottom. (b) ^{12}CO (J = 1–0) integrated intensity map of M 51 (Nakai et al. 1994), smoothed to the same spatial resolution (34″) as that of H I. The contour interval is 6.6 K km s^{-1}, and the intensity key is shown at the bottom. 10″ in the maps corresponds to a linear scale of 466 pc.

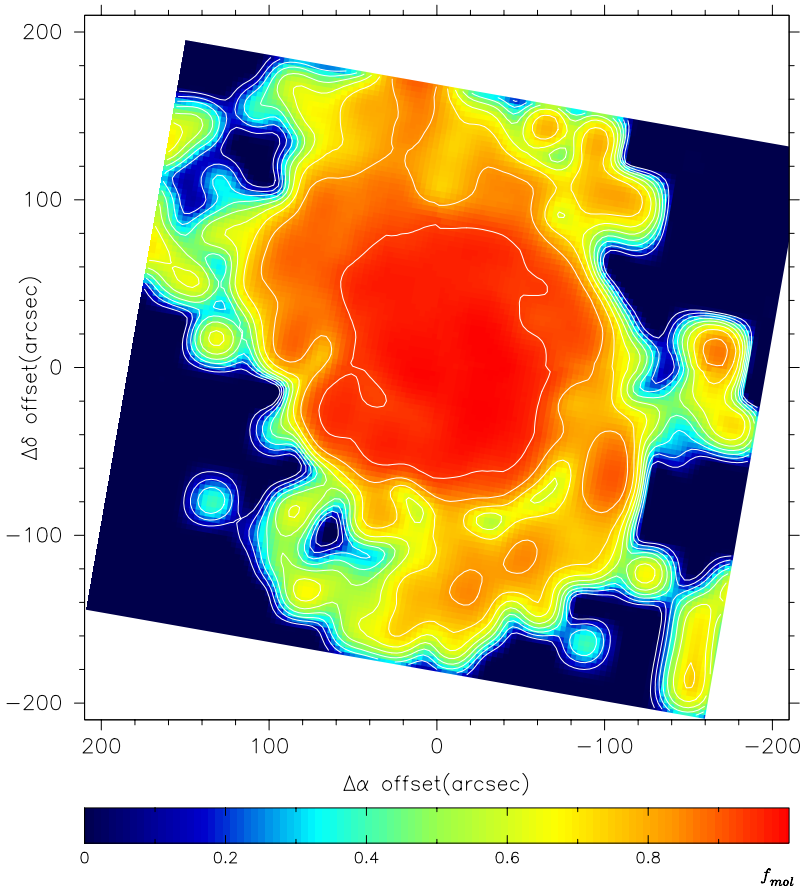

Fig. 2. Molecular fraction ($f_{\rm mol}$) in NGC 5194 (M 51). The contour levels are $f_{\rm mol}$ = 0.1, 0.2, ..., 0.9.

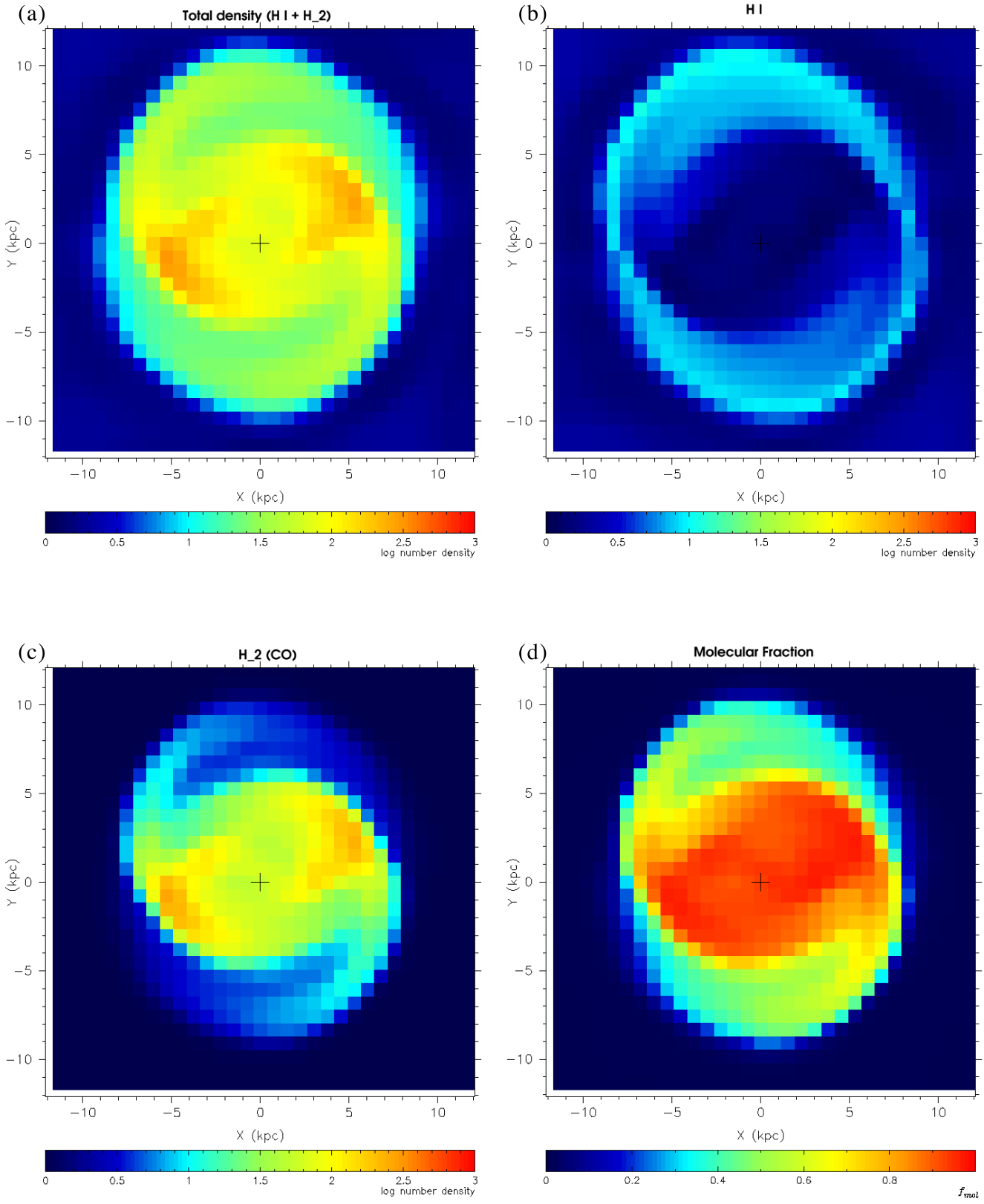

Fig. 3. (a) Snapshot of the numerically simulated total density distribution of interstellar gas. (b) The same for H I gas. (c) The same for H_2 molecular gas, simulating a CO-line intensity distribution. (d) Same as the molecular fraction, $f_{\rm mol}$. The value keys are shown at the bottom.

axisymmetric component, as given by

$$\Phi_0(R) = -\frac{c^2}{a}\frac{1}{(R^2 + a^2)^{1/2}}, \quad (5)$$

where a is the core radius, and $c = v_{\max}(27/4)^{1/4}a$, with $v_{\max}$ being the maximum rotation velocity. Through our numerical simulation, we fixed the core radius and maximum circular velocity to be $a = \sqrt{2}$ kpc and $v_{\max} = 200\,\mathrm{km\,s^{-1}}$.

The nonaxisymmetric potential was taken from Sanders (1977), assuming rigid rotation at a pattern speed, Ω_p, which has the form

$$\Phi_1(R, \phi) = \varepsilon\frac{aR^2}{(R^2 + a^2)^{3/2}}\Phi_0(R)\cos 2\left(\phi - \Omega_p t\right), \quad (6)$$

where ε is the strength of a bar of the order of $\varepsilon = 0.15$. Spiral shocked arms of gas are produced by this potential.

3.1.2. Initial condition

Initially, we set 256×256 two-dimensional cells corresponding to $12.8\,\mathrm{kpc} \times 12.8\,\mathrm{kpc}$ field, while setting the field center at the coordinate origin. The initial number density of the gas was taken to be $5\,\mathrm{cm^{-1}}$ for the inner disk at $R \leq 8\,\mathrm{kpc}$, and $1\,\mathrm{cm^{-1}}$ at $R > 8\,\mathrm{kpc}$. Initial rotation velocity of each gas cell was set so that the centrifugal force would balance the gravitation. The bar pattern speed, Ω_p, was taken to be $23\,\mathrm{km\,s^{-1}\,kpc^{-1}}$, and the strength of the bar, ε, was taken to be 0.10.

3.2. Elmegreen's Parameters

Following Honma et al. (1995), we represent U and Z by the following equations:

$$\frac{U}{U_\odot} = \exp\left(-\frac{R - R_{U_\odot}}{R_U}\right), \quad (7)$$

$$\frac{Z}{Z_\odot} = \exp\left(-\frac{R - R_{Z_\odot}}{R_Z}\right). \quad (8)$$

Here, R_U and R_Z are the scale radii of the radiation field and the metallicity, respectively, and $R_{U_\odot}$ and $R_{Z_\odot}$ are the radii at which the quantities are normalized to the solar values.

It is possible that the radiation field depends on the azimuthal direction, because star formation along the spiral arms is enhanced and newly born OB stars radiate strong UV emission. Thus, it seems that there is little UV radiation in the interarm regions. However, Greenawalt et al. (1998) presented deep Hα emission-line images of several spiral galaxies, including M 51, concluding that one half of the total Hα emission is attributed to diffusion of the ionized gas. This observation shows that the fluctuation of ionizing radiation field in the arm and interarm regions is not more than twice at their resolution of a few arcsecs. In the present simulation, the resolution was much lower, and the arm–interarm UV fields may be assumed to have an intensity fluctuation of less than twice: We here assume that the UV field is uniform along an azimuthal circle, and depends only on the galactocentric distance. Although they are beyond a scope of the present paper and will be a subject for simulations in the future, the variation in the radiation fields by star-forming arms should be taken into account, and UV radiation transfer through the arms, particularly through dark lanes, should be solved, in order to obtain a more realistic, higher resolution behavior of the molecular-fraction across spiral arms.

The interstellar pressure is estimated to be $P \propto \rho(\mathrm{gas})$ in the same manner as was done by Honma et al. (1995), and can be expressed by the following relation:

$$\frac{P}{P_\odot} \sim \frac{\rho}{\rho_\odot}. \quad (9)$$

We adopted the following normalizing parameters: $\rho_\odot = 2\,\mathrm{H\,cm^{-3}}$, $R_U = R_Z = 5.2\,\mathrm{kpc}$, and $R_{U_\odot} = R_{Z_\odot} = 11.5\,\mathrm{kpc}$. The latter two parameters are the same as those assumed by Honma et al. (1995). Although they assumed constant metallicity for NGC 5194, we assumed an exponential function as above (see e.g. Arimoto et al. 1996).

3.3. Simulated Spiral Molecular Front

Under these assumptions and initial conditions, we first calculated the time evolution of the distribution of the total gas. Figure 3a shows the density distribution after several galactic rotations. The density distribution in the initially uniform-density disk is strongly disturbed by the oval potential, and high-density arms are formed, which evolve into well-developed bisymmetric spiral arms. At the same time, the global radial density distribution is regulated to have a roughly exponentially decreasing structure. Inside the bar, straight high-density arms are formed along the axis of the bar, as well as many faint spiral-like arms. We are here interested in the global spiral pattern in order to compare with the observed gas density distributions, and do not discuss the smaller and fainter features, which will be finally smeared out when we compare the result with the observation.

The simulated distribution of gas density was, then, used to calculate the distribution of the gas pressure, P, which was further combined with the assumed distributions of the UV radiation field, U, and the metallicity, Z, as given above. Thus, we can calculated the molecular fraction at each grid point, and obtain a map of f_{mol}, as well as maps of atomic and molecular gases. Figures 3b, c, and d show snapshots of the thus-calculated maps for H I, H_2, and f_{mol}. In order to compare with the observations, we smooth the map of the molecular fraction by a Gaussian convolution, and compared it with an observation of M 51 at the same resolution as in figure 4.

4. Discussion

The simulated results can be summarized as follows. The detailed arm shapes were not well reproduced, because the simulation used a fixed bar-potential. In order for detailed arm features to be reproduced, we need to perform a self-gravitating N-body simulation, including both stars and gas, which is a subject for the future. However, the simulation depicted in figures 3 and 4 show a global agreement with the observations, and reproduces the following characteristics of the distribution of the molecular fraction in M 51. Around the nucleus f_{mol} is almost unity, and maintains a high value of $f_{\mathrm{mol}} > 0.8$ out to $r \sim$ kpc. At $r \sim 4$ to 5 kpc, f_{mol} decreases drastically to 0.4 or lower, and becomes nearly zero in the outer region. It is clear that the transition region, where f_{mol} is $\sim$0.5–0.6, is distributed

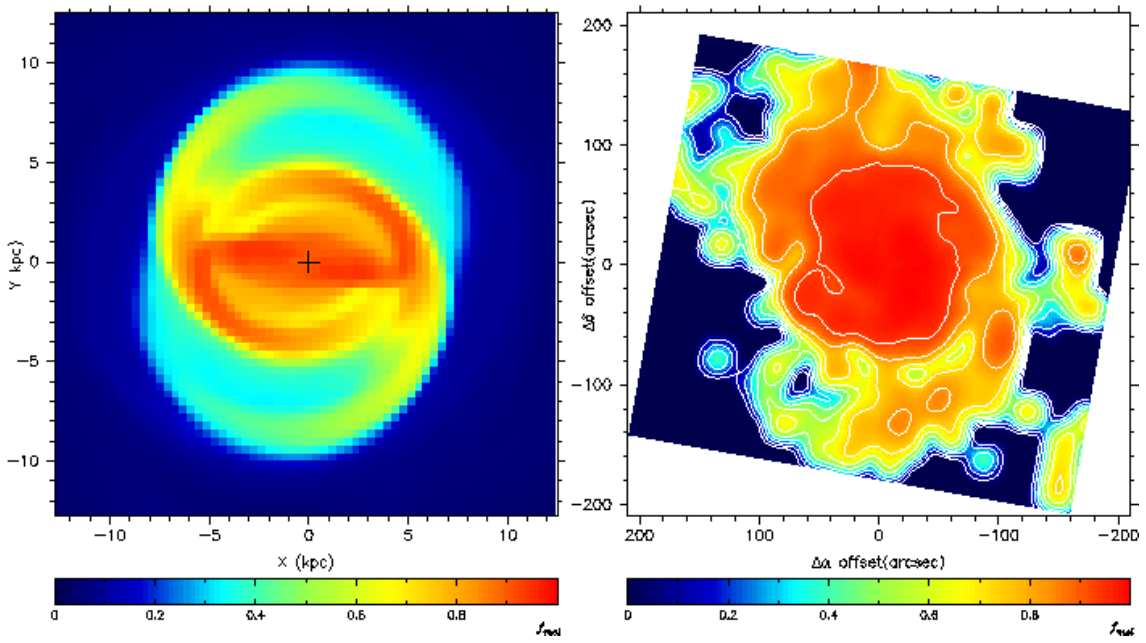

Fig. 4. Comparison of the simulated molecular fraction (left) smoothed to the same resolution as that of the observation of M 51 (right).

in a narrow annulus having a radius of 4.5 kpc, which means that the H I-to-H_2 transition occurs rather abruptly within a narrow range of the radius. This confirms the radial MF (Sofue et al. 1995; Honma et al. 1995).

In addition to the radial MF in the gas disk, azimuthal fluctuation of the molecular fraction is also significant. At $r \sim 6$ kpc, $f_{\rm mol}$ changes from nearly zero before encountering the arm to ~ 0.8 within ~ 200 pc in the azimuthal direction in the spiral arm. This narrow transition range corresponds to a time scale of ~ 2 Myr. This indicates that the molecular gas observed along spiral arms is formed only within ~ 2 Myr. This time scale is consistent with the H_2 forming time scale, $> 7 \times 10^5$ yr, predicted by Takahashi and Williams (2000) using a molecular-dynamics simulation.

On the other hand, the decaying time scale of molecular gas is longer, according to a more gradual decrease of the gas density after passage of the galactic shock. If we define a molecular arm as an armed region with $f_{\rm mol} > 0.5$, the width of the molecular arm is estimated to be ~ 2.5 kpc in the azimuthal direction. This corresponds to a lifetime of molecular gas of about 25 Myr, which is consistent with the semi-analytically calculated GMCs life time of ~ 40 Myr (Elmegreen 1991).

If we consider the radial variation of metallicity, Z, these local (arm) $f_{\rm mol}$ structures would depend on the galactocentric distance, even for the same gas density. Figure 3 shows that, for the same density of $\sim 5\,{\rm H\,cm^{-3}}$, the molecular fraction is ~ 0.5–0.6 in the inner interarm region, while it is 0.3–0.4 in the outer-arm regions. This reflects the fact that the molecular fraction depends not only on the gas density, but also on the strength of the radiation field and metallicity, particularly the latter.

We are grateful to Dr. M. Honma for helpful advice, and Mr. J. Koda for discussions on numerical simulations. The numerical simulations were performed using the VH-1 code developed by the numerical astrophysics group at the University of Virginia.

References

Arimoto, N., Sofue, Y., & Tsujimoto, T. 1996, PASJ, 48, 275
Blondin, J. H., & Lufkin, E. A. 1993, ApJS, 88, 589
Colella, P., & Woodward, P. R. 1984, J. Comp. Phys., 54, 174
Elmegreen, B. G. 1991, in The Physics of Star Formation and Early Stellar Evolution, ed. C. J. Lada & N. D. Kylafis (Dordrecht: Kluwer), 35
Elmegreen, B. G. 1993, ApJ, 411, 170
Greenawalt, B., Walterbos, R. A. M., Thilker, D., & Hoopes, C. G. 1998, ApJ, 506, 135
Honma, M., Sofue, Y., & Arimoto, N. 1995 A&A, 304, 1
Imamura, K, & Sofue, Y. 1997, A&A, 319, 1
Kuno, N., & Nakai, N. 1997, PASJ, 49, 279
Kuno, N., Nakai, N., Handa, T., & Sofue, Y. 1995, PASJ, 47, 745
Nakai, N., Kuno, N., Handa, T., & Sofue, Y. 1994, PASJ, 46, 527
Rots, A. H., Crane, P. C., Bosma, A., Athanassoula, E., & van der Hulst, J. M. 1990, AJ, 100, 387
Sanders, R. H. 1977 ApJ, 217, 916
Sofue, Y., Honma, M., & Arimoto, N. 1995, A&A, 296, 33
Takahashi, J., & Williams, D. A. 2000, MNRAS, 314, 273
Toomre, A. 1981, in The Structure and Evolution of Normal Galaxies, ed. S. M. Fall & D. Lynden-Bell (Cambridge: Cambridge Univ. Press), 111